 SDHM, vol.5, no.4, pp.311-335, 2009

A Strain-Based Constitutive Model for Concrete under Tension in Nonlinear Finite Element Analysis of RC Flexural Members

Smitha Gopinath[1], J. Rajasankar[1,2], Nagesh R. Iyer[1], T. S. Krishnamoorthy[1] B.H. Bharatkumar[1] and N. Lakshmanan[1]

Abstract: In this paper, a two-phase strain-based constitutive model is proposed for concrete under tension. First phase deals with modelling uncracked concrete while the behaviour of concrete in cracked condition is modelled in second phase with appropriate theoretical support. A bilinear tension softening curve of concrete defined in crack width-stress space is taken as the basis to propose the model. Smeared representation of reinforcement and cracks along with multi-layered geometry definition of reinforced concrete (RC) structures is used to implement the model. Through this, it is shown that change in the orientation of tensile cracks with increasing load on the structure can be accounted. Stress transfer between cracked concrete and reinforcing bar is made use of to model the slip between them. By applying energy equivalence principle, simple expressions are derived for crack width as function of strain and fracture energy of concrete. For validation of the model and other associated features, two sample RC structures are analysed for their nonlinear response up to ultimate state. Computed responses are found to match closely with those obtained in experiments conducted by the authors and others. Through this, superior performance of the proposed model to evaluate the nonlinear response of RC flexural members is demonstrated.

Keywords: Reinforced concrete structures; Nonlinear finite element analysis; Tension softening; Constitutive model; Crack width; Bond-slip

1 Introduction

Nonlinear behaviour of reinforced concrete (RC) structures arise primarily due to local phenomena such as bond-slip, aggregate interlock, dowel action and tension softening (Assan 2002) which are directly associated with cracking of concrete un-

[1] CSIR, Structural Engineering Research Centre, Taramani, Chennai 600113, India
[2] Corresponding author E-mail: sankar@sercm.org

der tension. Softening behaviour of concrete on reaching threshold tensile strain can be defined by linear (Hillerborg et al. 1976), bilinear (Petersson 1981), exponential (CEB-FIP 1990) or hyperbolic law (Frag and Leach 1996; Kratzig et al. 2004). In fact, different values for parameters of a bilinear model lead to different shapes of softening curve. Roesler et al. (2007) have derived a bilinear softening model from measured fracture properties of concrete and implemented in a finite element- based cohesive zone model (CZM). It, however, restricts crack propagation to be modelled only in vertical direction along a predetermined path. Among the experimental fracture parameters of concrete, initial fracture energy (g_f) and tensile strength (f_{ct}) are found to contribute significantly to the peak load, whereas the total fracture energy (g_F) influences the post-peak response behaviour. Direct tension tests can also be used (Reinhardt et al. 1986) to arrive at a suitable expression for softening of concrete.

Once a crack is formed, its propagation plays important role in deciding the nonlinear response of RC structures. Change in crack direction affects the stiffness of RC members, especially when the applied load is close to ultimate strength of the structure. Experimental evidence is available (Vecchio and Collins 1986) to show that the direction of crack extension changes with loading history and similarly the response of a structure depends strongly on current crack direction. Rotating crack model due to Gupta and Akbar (1984) restricts the crack direction to be perpendicular to maximum principal tensile strain direction. Direct correlation of the attributes of principal tensile strain with the crack characteristics is an attractive feature of this model which is found to be capable of predicting the nonlinear response of a variety of RC structures after cracking (Cerioni et al. 2008). Due to such positive features, this crack direction model has been used in the present study to describe the orientation of cracks. Simple expressions available in design standards (IS-456 2000; BS:8110 1989; ACI:318 1984) to calculate the maximum crack width are based on theory of bending. Utmost, crack width is computed as function of an assumed average crack spacing and strain in reinforcing bar (Chowdhury 2001; Vidal et al. 2004; Malecki et al. 2007). Even recently, Theiner and Hofstetter (2009) have used such expressions to predict crack width in concrete structures. To the best of the author's knowledge, no formulation is available which evaluates crack width directly using the results of nonlinear finite element analysis of RC structures. To fill this gap, a new methodology is proposed for crack width calculation and its potential is explored through numerical studies.

Establishing bond-slip relation for reinforcing bars based on experiments is extremely difficult, since measured values generally represent the average over gauge length. In spite of this, a number of bond-slip relations were proposed in literature (ASCE 1982; Eligehausen et al. 1983; Hayashi and Kokusho 1985). To account

for the bond-slip of reinforcement, link element (Oliveira et al. 2008; Russo et al. 2009) is preferred when overall structural behaviour is the primary interest. This, however, imposes restrictions in terms of finite element mesh grading and twin nodes at concrete-steel interface. To avoid these restrictions, a novel bond-slip model is used that allows direct consideration of nonlinear bond–slip relation. It performs in contrast to the approaches available for the transition of concrete-reinforcement interaction from bar scale to member (structural) scale (Lackner et al. 2003). Necessary computations were performed at the bar scale level in advance to arrive at the calibration parameters required at the member scale level. Hence, no additional information is needed during structural analysis at the member scale, rendering a robust material model for analysis of RC structures. Bond-slip effect along the reinforcing bar is quantified using force equilibrium and compatibility conditions in the post-cracking stage.

Through this paper, a new two-phase constitutive model is proposed for concrete under tension. Concrete is modelled to show linear behaviour till its tensile strain exceeds its cracking strain capacity. Concrete behaviour after cracking is defined by a bilinear softening law on the basis of stress-strain description. Motivation for the proposed constitutive model is due to a softening law by Petersson (1981) but in terms of tensile stress and crack width. The model is integrated with layered geometry definition of RC structures to accommodate continuously changing crack direction while progressing through thickness. To aid in serviceability verification of RC structures, an expression has been derived for crack width as function of concrete strain and fracture energy by applying energy equivalence principle. Proposed crack width expression presents significant advantage over those available in literature by not depending on an estimate of average crack spacing. Instead, strains computed from conventional nonlinear finite element analysis and fracture energy of concrete determined from an experiment are directly used to calculate the crack width. To the best of author's knowledge, such an attempt for the prediction of crack width has not yet been reported in literature till date. Further, a bond-slip model is used by combining the equilibrium conditions with the bond model of CEB-FIP (1990). In both the studies, performance of the proposed constitutive model in conjunction with other associated features was verified by analysing two simple RC structures. In both the studies, predicted nonlinear responses are found to compare well with corresponding values measured in experiments including that conducted by authors earlier.

2 Constitutive Model for Concrete in Tension

Concrete is treated as quasi-brittle material under tension and, accordingly, a two-phase constitutive model, viz., pre-cracking and post-cracking (Fig. 1) is proposed.

Among these, modelling the post-cracking phase is crucial in nonlinear analysis of RC structures and is taken as primary focus of the present paper. A strain-based cracking criterion and a bilinear softening curve are critical elements of the constitutive model. While developing the model, structural behaviour of RC members is approximated by plane stress condition and so 4-noded isoparametric plane stress element (Au and Bai 2007) is used to represent the geometry.

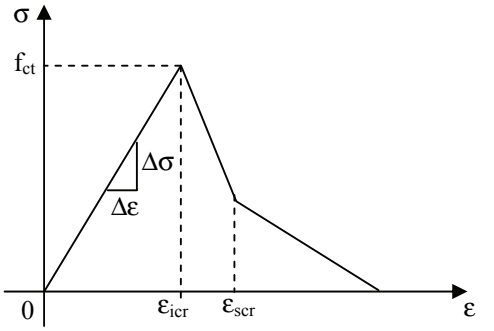

Pre-cracking phase
- No cracks
- Isotropic, homogenous material model
- Linear behaviour

Post-cracking phase
- Tensile cracks
- Orthotropic material model
- Nonlinear behaviour

Figure 1: Two-phase constitutive model for concrete in tension

2.1 Pre-cracking Phase

With reference to Fig. 1, concrete is modelled as homogenous and isotropic material in uncracked state. Based on this, linear behaviour is assumed for concrete till reaching the cracking surface. A strain-based state identification criterion is used as part of the proposed model. Eqns. (1a) and (1b) state the criterion as

$$0 < \varepsilon \leq \varepsilon_{icr} : \text{ Pre - cracking phase} \tag{1a}$$

$$\varepsilon \geq \varepsilon_{icr} : \text{ Post - cracking phase} \tag{1b}$$

where ε and ε_{icr} are, respectively, tensile strain and corresponding capacity of concrete against cracking. In pre-cracking phase, 2-D stress state is defined simply by

$$\Delta\sigma = D\Delta\varepsilon \tag{2}$$

where

$$\{\Delta\sigma\}^T = \{\Delta\sigma_{xx}, \Delta\sigma_{yy}, \Delta\tau_{xy}\} \tag{3}$$

$$\{\Delta\varepsilon\}^T = \{\Delta\varepsilon_{xx}, \Delta\varepsilon_{yy}, \Delta\gamma_{xy}\} \tag{4}$$

$$D = D_0 = \frac{E}{1-\nu^2}\begin{bmatrix} 1 & \nu & 0 \\ \nu & 1 & 0 \\ 0 & 0 & \frac{1-\nu}{2} \end{bmatrix} \tag{5}$$

E and ν are elastic modulus and Poisson's ratio of concrete in tension; x- and y- are orthogonal global directions and D_0 is the constitutive matrix; σ_{ij} and ε_{ij} for i, j = x and y are two-dimensional normal stress and strain components in concrete; τ_{xy} and γ_{xy} are shear stress and shear strain components. In the above, stress-strain relation is defined by plane stress condition.

2.2 Post-cracking Phase

Characteristics of cracks and its effects on the structural behaviour of RC are modelled in post-cracking phase. Basically, the strain-based cracking criterion mentioned in Eqn. (1b) is used to activate this phase beyond which concrete behaviour is proposed to be modelled by using a bilinear softening curve. An, existing tension softening curve (Petersson 1981; Xu 2000) is used as basis for the proposal. The softening curve shown in Fig. 2(a) is described in terms of tensile stress in concrete (σ) and crack width (w) by Petersson (1981) as

$$\sigma = f_{ct} - (f_{ct} - \sigma_s)\frac{w}{w_s} \text{ for } 0 \le w \le w_s \tag{6}$$

$$= \sigma_s \frac{w_0 - w}{w_0 - w_s} \text{ for } w_s < w \le w_0 \tag{7}$$

$$= 0 \text{ for } w > w_0 \tag{8}$$

Unique definition of the curve is realized by using following parameters: tensile strength of concrete (f_{ct}), transition points (σ_s, w_s) and maximum crack width (w_0) at which stress reduces to zero. Among these, tensile strength of concrete can be determined through simple experiment and other parameters were expressed as empirical relations based on tensile strength (Petersson 1981) as

$$\sigma_s = \frac{f_{ct}}{3} \tag{9}$$

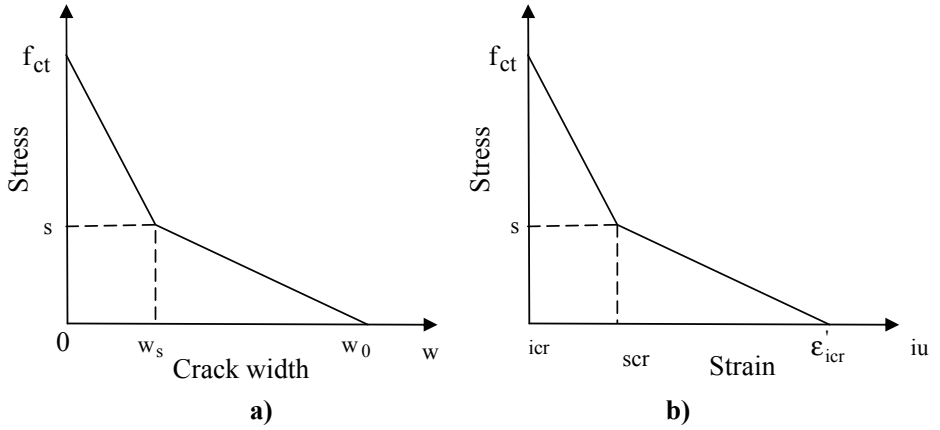

Figure 2: Bilinear tension softening curve (a) in σ-w (after Petersson, 1981) (b) in σ-ε (proposed)

$$w_s = \frac{0.8G_F}{f_{ct}} \tag{10}$$

$$w_0 = \frac{3.6G_F}{f_{ct}} \tag{11}$$

In Eqns. (10-11), fracture energy of concrete, g_F, is given by (CEB-FIP 1990)

$$G_F(in\ N/mm) = G_{F0}\left(\frac{f_{cm}}{f_{cm0}}\right)^{0.7} \tag{12}$$

where
f_{cm} is the mean compressive strength of concrete in N/mm^2
f_{cm0}= 10 N/mm^2 for $f_{cm} \leq$ 80 N/mm^2
g_{F0}= 0.0204+$\frac{0.0053(d_{max})^{0.95}}{8}$ N/mm
d_{max}= maximum size of aggregate in mm

Xu (2000) has investigated the parameters of the bilinear softening curve and provided their physical interpretation based on extensive numerical studies. Practical application of this softening curve is, however, limited due to its dependence on crack width whose calculation is somewhat involved. To alleviate this limitation, and also as a contribution of this paper crack width is replaced by strains in the tension softening curve. In that case, tension softening effect can be directly computed in a conventional nonlinear finite element analysis of RC structures in which strain

is modelled as field variable. By doing so, the bilinear softening curve will have wider application along with ease of implementation. In this background, Eqns. (9) and (10) are submitted into Eqn. (6) to express the tensile stress as

$$\sigma = \frac{f_{ct}}{2}\left[\frac{2\varepsilon_{icr} - \varepsilon_{iu}}{\varepsilon_{icr}}\right] \text{ for } \varepsilon_{icr} < \varepsilon_{iu} \leq \varepsilon_{scr} \tag{13}$$

By making use of Eqns. (10) and (11), stress in the strain range ε_{scr} to ε'_{icr} is expressed as

$$\sigma = \frac{f_{ct}}{3}\left[\frac{\varepsilon'_{icr} - \varepsilon_{iu}}{\varepsilon'_{icr} - \varepsilon_{scr}}\right] \text{ for } \varepsilon_{scr} < \varepsilon_{iu} < \varepsilon'_{icr} \tag{14}$$

By taking inspiration from Eqn. (8), tensile stress is reduced to zero for critical strain value equal to ε'_{icr}. The value of critical strain is taken as twice of cracking strain, i.e., $\varepsilon'_{icr} = 2\varepsilon_{icr}$. Based on experiments using specimens, Cho et al. (2003) have reported exponential stress-strain behaviour for concrete in tension with maximum strain nearly four times the cracking strain. However, in the present bilinear model, the maximum strain in post-cracking range has been fixed as two by considering equivalent area under the stress-strain curve. Further, by imposing continuity conditions between Eqns. (13) and (14), transition point is located on strain axis as

$$\varepsilon_{scr} = \frac{4}{3}\varepsilon_{icr} \tag{15}$$

The resulting softening curve is available in Fig. 2(b).

2.2.1 Cracked concrete model

Concrete is assumed to be cracked when the strain criterion given in Eqn. (1b) is satisfied. Cracks are modelled to form perpendicular to the direction of maximum principal tensile stress (Cerioni et al. 2008). After cracking, concrete behaviour is modelled to be orthotropic (Ramtani et al. 1992; Cervera 2008) for monotonic increase in applied load, cracks tend to progressively grow which induce corresponding increase in orthotropic character of cracked concrete. In addition, the internal stress distribution in the member is modified dynamically to satisfy equilibrium. After cracking, the load carried by concrete is gradually transferred to reinforcing steel which starts yielding after the stress in steel reach the yield value. This simultaneously introduces change in crack direction. Cracks are reoriented at every load level to maintain strict perpendicularity with the direction of maximum principal stress. To facilitate this, a composite layered geometry is adopted for plane stress finite element (Figs. 3a and 3b).

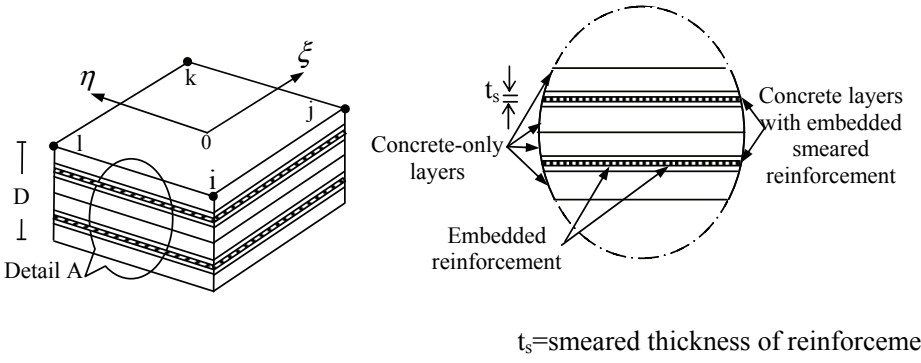

Figure 3: a) Layer representation of a plane stress finite element; b) Detail A

Stress-strain relation of reinforcement is modelled as uniaxial described by bilinear curve which includes strain hardening (Assan 2002). Geometrical representation of reinforcement is done by invoking smeared concept (ASCE 1982) and inserted into selective concrete layers of a finite element (Fig. 3b). For uniform reinforcement in a cross section, smeared thickness (t_s) is determined as ratio of a bar (A_{s1}) to bar spacing (b_s). By similar means, smeared thickness can be obtained for non uniform reinforcement also.

In order to have better representation of cracked behaviour, the proposed model can accommodate independent cracks at each of the integration points in a finite element. For example, the 4-noded bilinear finite element shown in Fig. 4 can hold four cracks at each of the integration points. Angle of each crack is evaluated separately as function of the local stress field after satisfying normality condition with the principal stress. With respect to Fig. 4, angle of a crack with y-axis is

$$2\alpha_1 = Tan^{-1}\left[\frac{2\tau_{xy}}{\sigma_{xx}-\sigma_{yy}}\right] \tag{16}$$

Finally, material matrix of a finite element is calculated as an average of that represented by the four integration points in the element. Further steps to calculate the stiffness matrix of an element is a standard exercise in finite element analysis (Zienkiewicz and Taylor, 2000) and, therefore, not discussed here.

Characteristics of proposed model enable accounting the interaction between crack characteristics and redistribution of internal stresses as schematically shown in Fig. 5. Concrete is modelled to resist only the compressive force parallel to a crack while forces normal to the crack are resisted by reinforcement. In post-cracking phase also Eqn. (2) is valid to define the stress state in the structure except for the

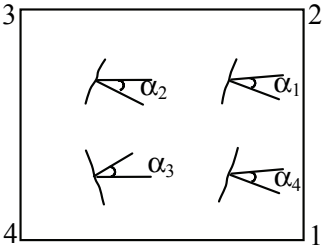

Figure 4: Cracks at integration points in a 4-noded bilinear finite element

constitutive matrix definition as

$$D = [D_0] + [D_{cr}] \tag{17}$$

where

$$[D_{cr}] = [G] = \frac{-\sigma_2}{2\sqrt{(\varepsilon_{xx} - \varepsilon_{yy})^2 + \varepsilon_{xy}^2}} \begin{bmatrix} sin^2 2\alpha_1 & -sin^2 2\alpha_1 & -cos2\alpha_1 sin2\alpha_1 \\ & sin^2 2\alpha_1 & sin2\alpha_1 cos2\alpha_1 \\ symm & & cos^2 2\alpha_1 \end{bmatrix} \tag{18}$$

σ_2 is the minor principal stress
ε_{xx}, ε_{yy} and γ_{xy} are normal and shear strain components.
Obviously, the additional material matrix, D_{cr} introduces the contribution of a crack in terms of its orientation to the response of concrete.

3 Crack Width

Maximum crack width is widely used to verify the serviceability of RC structures (IS-456 2000; BS:8110 1989; ACI:318 1984). Few crack width expressions are available due to experimental recordings (Colotti and Spadea 2005; Malecki et al. 2007). These expressions mainly address flexural beams and, therefore, derived as function of gross structural parameters such as cover thickness, stress in steel and spatial distribution of longitudinal reinforcement. In finite element analysis, commonly crack width is calculated by multiplying average crack spacing and the predicted strain values (Malecki et al. 2007). Major limitation in using average crack spacing is its variation for a variety of conditions. As a remedial measure, an expression has been derived for crack width as a function of tension softening response of concrete. For this, equivalence of energy between traction-separation proposed by Petersson (1981) and the stress-strain based softening curve proposed in this paper are used. By equating the stress in post-cracking phase as given by

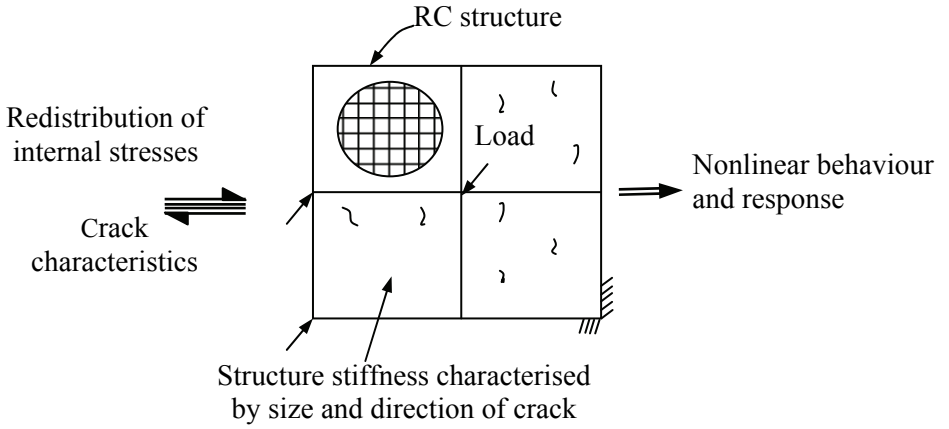

Figure 5: Interaction between crack characteristics and redistribution of internal stresses in a RC structure

Eqns. (6) and (13) and also making use of Eqns. (9) and (10), an expression for crack width in medium strain range is derived as

$$w = \frac{0.6G_F}{f_{ct}} \left[\frac{\varepsilon_{iu}}{\varepsilon_{icr}} \right] \text{ for } \varepsilon_{icr} < \varepsilon_{iu} \leq \varepsilon_{scr} \tag{19}$$

In the same way, by comparing Eqns. (7) and (14), with the support of Eqns. (9) and (11), an expression for crack width in higher strain range is derived as

$$w = \frac{G_F}{f_{ct}} \left[\frac{10.8\,\varepsilon'_{icr} - 14.4\varepsilon_{icr} + 8.4\varepsilon_{iu}}{3\,(\varepsilon'_{icr} - 4\varepsilon_{icr})} \right] \text{ for } \varepsilon_{scr} < \varepsilon_{iu} \leq \varepsilon'_{icr} \tag{20}$$

Attractive feature of the crack width expressions in Eqns. (19) and (20) is their dependence only on the computed strain values. Elimination of traction-separation behaviour of concrete in tension brings in the much-needed simplification in the calculations over the most widely followed (CEB-FIP 1990). Further, as strains are predicted in a finite element analysis by accounting for a variety of geometry, loading and material conditions, the expressions derived in Eqns. (19) and (20) are considered to be more general in nature. As strains are fundamental to describe the material state, the proposed crack width expressions are expected to be reliable.

4 Bond-Slip

A compatible bond-slip model has been integrated with the constitutive model to include the effects of load transfer from concrete to reinforcement after cracking.

The model has been devised in such a way to activate the load transfer upon satisfying the tensile cracking criterion given in Eqn. (1b). Load transferred through bond is stipulated to be proportional to the difference in strain between concrete and reinforcement. Basic relations of the one-dimensional stress transfer are elucidated using differential elements in Fig. 6.

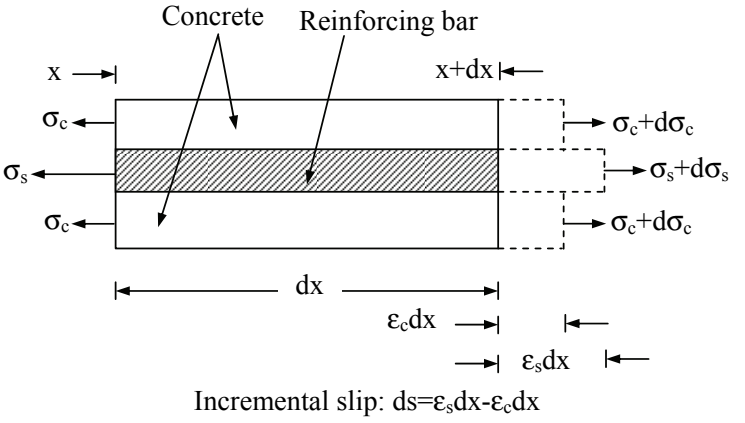

Figure 6: Equilibrium condition for bond-slip

Force equilibrium of the differential reinforcing element in Fig. 6 is written as

$$d\sigma_s(x)A_s = \tau_b(x)U_s dx \tag{21}$$

where

τ_b is the bond stress
U_s and A_s are the perimeter and cross sectional area of the reinforcing bar

Similarly, force equilibrium of the differential concrete element is written as

$$d\sigma_c(x)A_{c,eff} = -d\sigma_s(x)A_s \tag{22}$$

where $A_{c,eff}$ is the effective sectional area of the concrete participating in load transfer.

Slip is defined as difference between elongation of reinforcement (v_s) and concrete (v_c). As steel has better elongation capabilities, it is expressed as

$$s(x) = v_s(x) - v_c(x) \tag{23}$$

Representing Eqn. (23) in differential form,

$$\frac{ds(x)}{dx} = \frac{dv_s(x)}{dx} - \frac{dv_c(x)}{dx} \tag{24}$$

$$= \varepsilon_s - \varepsilon_c \tag{25}$$

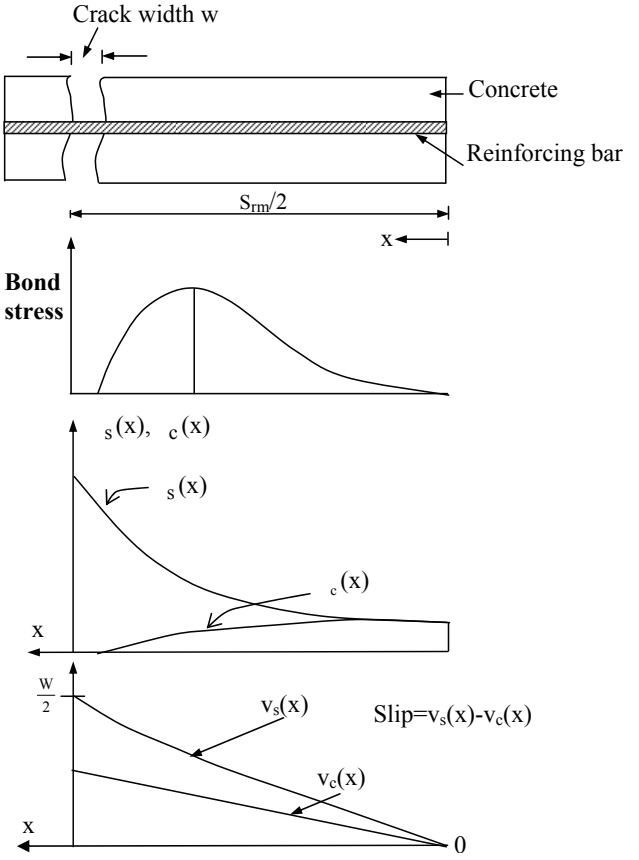

Figure 7: Details of bond-slip model

A sample tensile crack, stress distribution due to it in concrete and steel are shown in Fig. 7. On the basis of assumed crack spacing (S_{rm}), and also using Eqns. (21-25), following expressions are derived

$$\sigma_s(x) = \sigma_s(x=0) + \frac{U_s}{A_s} \int_0^{s_{rm}/2} \tau_b(x)dx \tag{26}$$

$$\sigma_c(x) = \sigma_c(x=0) - (\sigma_s(x) - \sigma_s(x=0)) \frac{A_s}{A_{c,eff}} \tag{27}$$

$$s(x) = \int_{x=0}^{s_{rm}/2} \varepsilon_s(x)dx - \int_{x=0}^{s_{rm}/2} \varepsilon_c(x)dx \tag{28}$$

Crack spacing advocated by CEB-FIP (1990) is used in the implementation. As per that

$$s_{rm} = \frac{2}{3}\frac{d_s}{3.6\rho_{s,eff}} \tag{29}$$

where
d_s = diameter of reinforcing bar and $\rho_{s,eff} = A_s/A_{c,eff}$
Similarly the bond model shown in Fig. 8 (CEB-FIP 1990) is used to define the distribution of bond stress. The relation adopted in present study is based on similar values measured from experiments.
According to Fig. 8,

$$\tau_b(s) = \tau_{max}\left(\frac{s}{s_1}\right)^{\alpha} \text{ for } 0 \le s \le s_1 \tag{30}$$

$$\tau_b(s) = \tau_{max} - (\tau_{max} - \tau_f)\left(\frac{s - s_1}{s_3 - s_1}\right) \text{ for } s_1 < s \le s_3 \tag{31}$$

$$\tau_b(s) = \tau_f \text{ for } s > s_3 \tag{32}$$

Values of model parameters for concrete in unconfined condition are suggested (CEB-FIP 1990) as s_1=0.6mm, s_3=1.0mm, α=0.4, $\tau_{max} = 2\sqrt{f_{ck}}$ and $\tau_f = 0.15\ \tau_{max}$. These values are used in model validation in the next section.

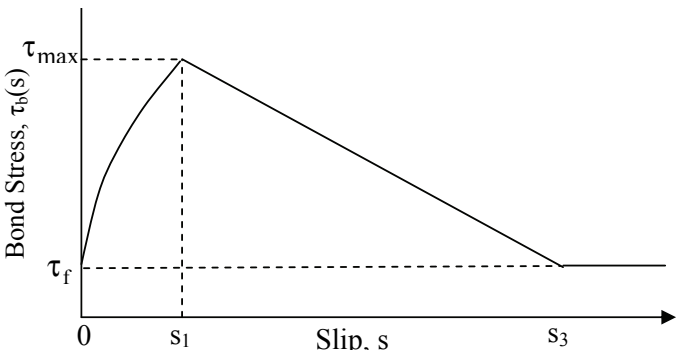

Figure 8: Bond stress-slip relation for unconfined concrete (from CEB-FIP 1990)

5 Model Validation

Two experimentally tested RC flexural members are analysed to verify the performance of tension softening model and other associated modelling strategies described in this paper. First is a simply supported RC beam and it has been analysed for two point loading to secure a short span that experiences only flexure. Computed nonlinear response up to ultimate load is compared with that of experiment conducted by authors. Second is the McNeice slab (Zhang et al. 2007) which is analysed for a central point load and the nonlinear response is verified against that of experiment and numerical studies available in literature. Load-displacement behaviour of the tested members beyond ultimate load and cracking response are used as key parameters to assess the performance of the models. Based on the model described in this paper, present analysis is expected to produce better comparison with results obtained from other comparable strategies about the state of the RC structure.

5.1 Example 1: Nonlinear analysis of a simply supported beam

Results of the simply supported RC beam tested by the authors are used to validate the models. Nonlinear response of the beam is evaluated for the standard two-point loading with the aim to realize a pure flexure zone at the mid span. Due to this, non linear analysis of the beam presents an ideal case to observe the pattern and characteristics of cracks with the aim to assess the performance of models responsible to this. Cross-section of the beam is 150mmx300mm while the length is 3.0m (Fig. 9).

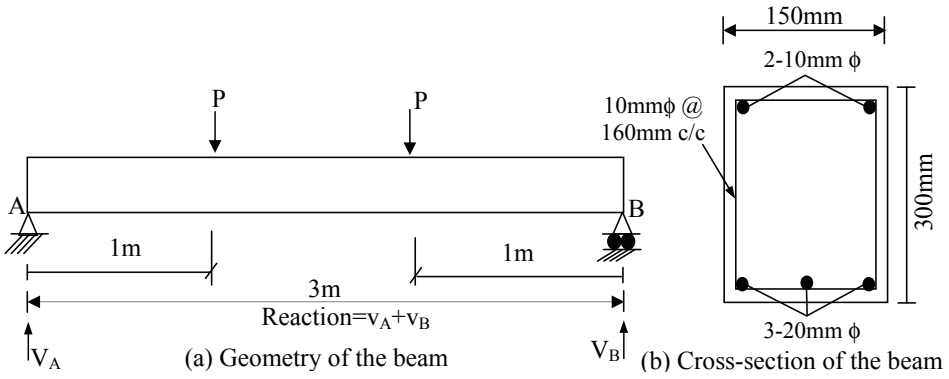

Figure 9: Details of beam

Laboratory tests on concrete specimens at 28 days showed a compressive strength

of 40 MPa while the yield strength of reinforcing steel is 415 MPa. Design of the beam is done as per IS-456 (2000) to arrive at a balanced section which requires about 2% steel in tension region. Capacity design principles are applied to ensure that the beam encounters only flexural failure mode. During testing, the beam is subjected to two-point loading as shown in Fig. 9. Among other responses, deflection at load points and also at mid-span are measured to characterize the nonlinear behaviour of the beam.

Table 1: Material properties of beam

Concrete				**Reinforcement**		
f'_c(MPa)	E_c(MPa)	f_{ct}(MPa)	ε_{cu}	ε_{su}	f_y(MPa)	E_s(MPa)
70.1	38500	3.67	0.004	0.15	415.0	$2x10^5$

The beam is analysed for its response by using the proposed modelling approach. Geometry and material characteristics of the beam available in Fig. 9 and Table 1 are utilised to build the finite element model. Apart from the load-deflection response, width of flexural cracks is computed according to the method described in Section 3.

Taking advantage of symmetry, only half the beam has been discretised using ten 4-noded shell elements. Cross-section of the beam is represented by 6 layers of each 50 mm thick. Among these, 2 layers are embedded with smeared reinforcement properties corresponding to top and bottom reinforcement. Remaining layers are retained as pure concrete layers. Equivalent thickness of smeared reinforcement at top and bottom are calculated, respectively, as 0.654mm and 5.23mm. Shear reinforcement is incorporated into the model by way of enhancing the shear stiffness of the finite elements (Hwang and Yun 2004; Gomes and Awruch 2001). Beam is analysed by imposing displacements at designated nodes in the finite element model. Sum of reactions realized at the two supports is taken as the load required to produce the imposed deflection at any stage of loading.

Variation of deflection at centre of the beam against the reaction is shown in Fig. 10. Corresponding values due to experiment are presented in the same figure for comparison, Predicted deflection behaviour is found to closely follow the measured values in both linear and nonlinear range up to reaching the ultimate value. Even in post-ultimate range, the proposed models are found to perform satisfactorily considering the uncertainly involved in behaviour modelling of RC structures. Analysis predicted an ultimate load of 212kN for the beam while the same is found to be 215kN from experiment. Thus, the superior performance of the model is verified. Maximum crack width calculated at different load levels in all the finite

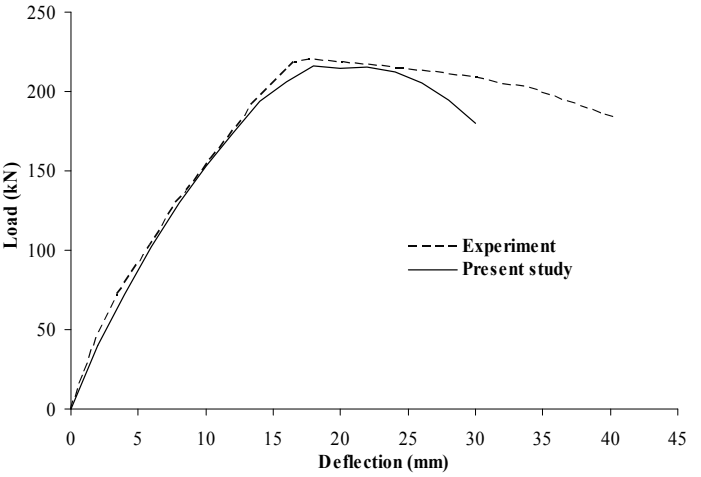

Figure 10: Load vs deflection at centre of the beam

elements in the pure flexure zone is shown in Fig. 11. As indicated earlier, absence of shear is the sole criterion based on which the central zone is chosen to verify the crack width prediction models. It is expected to have better comparison for the crack width as it is governed only by flexure. From the figure, it can easily be noted that cracks having a width of more than 0.05mm are formed as early as 30% of ultimate load. Maximum crack width at ultimate load is calculated as 0.2mm while it is measured in experiment as 0.18mm. Table 2 gives details about the predicted behaviour of all the elements in the flexure zone.

Bond stress-slip variation is plotted in Fig. 12 for the complete load range. Highly nonlinear behaviour is observed particularly near the peak values. This local behaviour is one of the major contributors to the overall nonlinear behaviour of the beam. As an approximate guideline, slip is not expected for low bond stress values in the range $0.2f_{ct}$ to $0.8f_{ct}$ while it could be of noticeable value in the bond stress range of $0.8f_{ct}$ to f_{ct}. Higher values of bond stress are accompanied by appreciable slip which is the cause for severe nonlinearity in the structural response. Depending on the quality of bond, the values mentioned above may marginally vary.

5.2 Example 2: Analysis of McNeice Slab for nonlinear response

Measured and predicted responses of McNeice slab (Zhang et al. 2007) are used to verify the performance of proposed models. Geometry, reinforcement and cross-section of the slab are shown in Fig. 13 and the material properties are listed in

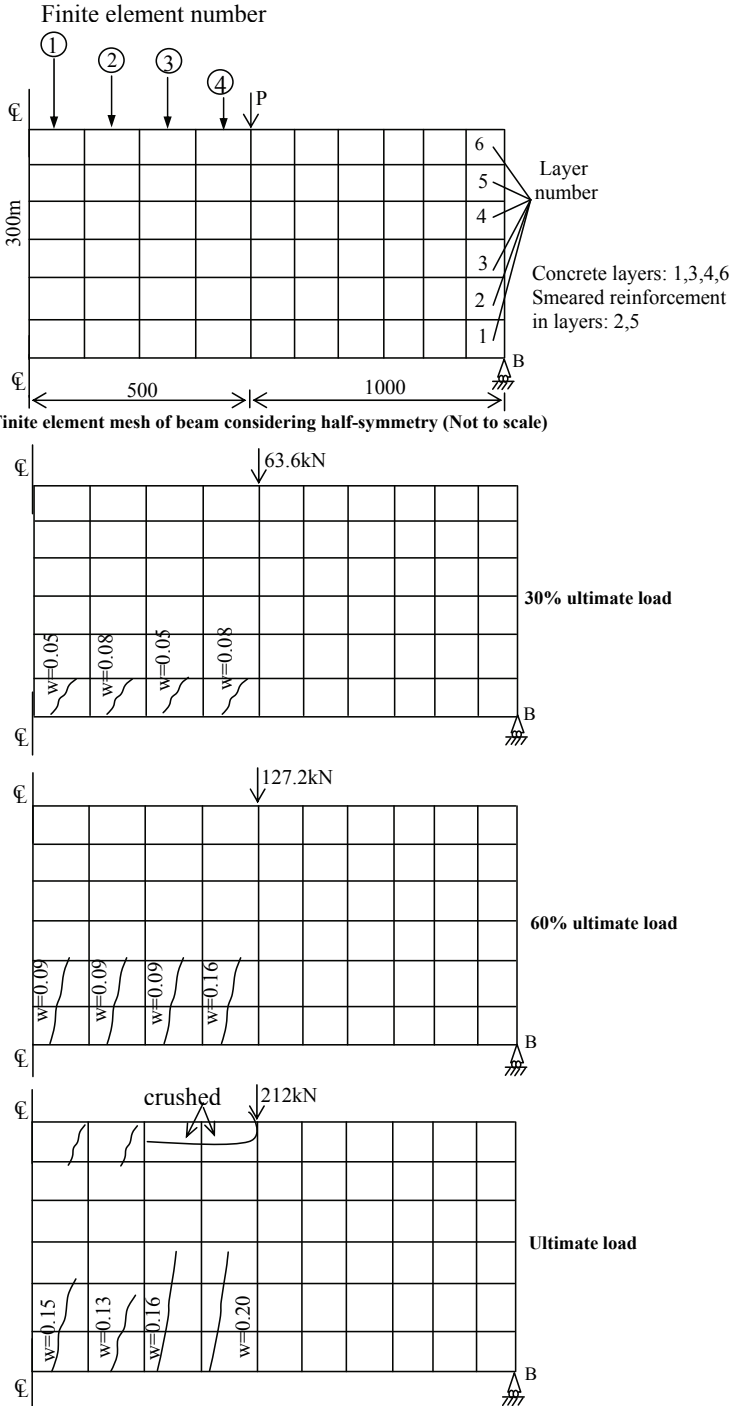

Figure 11: Crack width (in mm) in central zone elements

Table 2: Cracking details in elements 1, 2, 3 and 4

Element No.	Load (kN)	Layer No					
		1 Bottom	2	3	4	5	6 Top
1	36.8	x					
2		x					
3		x					
4		x					
1	71.4	x					
2		x					
3		x					
4		x					
1	102	x					
2		x					
3		x	x				
4		x	x				
1	130.2	x	x				
2		x	x				
3		x	x				
4		x	x				
1	153.8	x	x				
2		x	x				
3		x	x				
4		x	x				
1	173.4	x	x				
2		x	x				
3		x	x				
4		x	x				
1	194.2	x	x				
2		x	x				
3		x	x				
4		x	x				
1	206	x	x				
2		x	x				
3		x	x	x		o	o
4		x	x	x		o	o
1	212	x	x				
2		x	x				
3		x	x	x	x	o	o
4		x	x	x	x	o	o

x - cracking of concrete
o - crushing of concrete

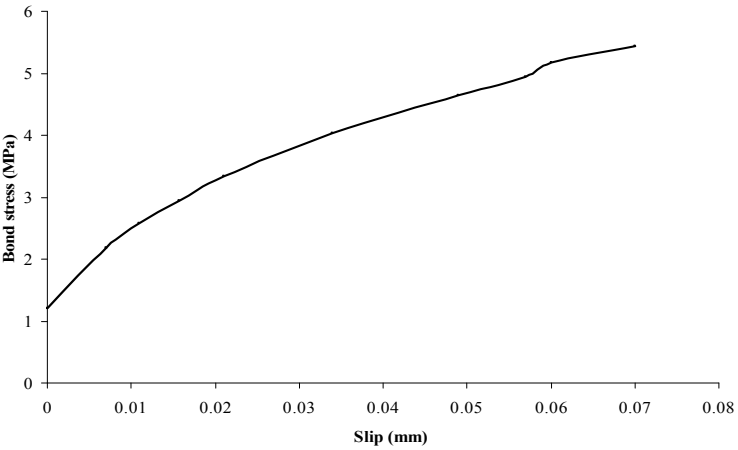

Figure 12: Bond stress -slip variation in simply supported beam

Table 3. Only one quarter of the slab is discretised by using a 3x3 non-uniform mesh as shown in Fig. 13. Thickness of the slab is represented by six layers among which one layer is embedded with smeared reinforcement. Nonlinear analysis is carried out for displacement controlled loading and with the aim to find the response behaviour and ultimate load. Slab response is monitored at each load step by the vertical displacement of node 2 for enforced displacement at the centre of the slab. Choice of location for loading and measurement is dictated by the reported response measurements made on the slab (Zhang et al. 2007). Computed nonlinear displacement response of the slab has been compared with that of experiment in Fig. 14. The present model has been found to predict post-ultimate response of the slab as shown in Fig. 14 whereas Zhang et al. (2007) have reported similar response only up to ultimate load.

Table 3: Material properties for McNeice slab

Material Properties	**Concrete**	**Reinforcement**
Elastic modulus kN/mm^2	E$_c$=28.6	E$_{s=}$200
Poisson's ratio	$\nu_c = 0.15$	$\nu_s = 0.3$
Yield stress, N/mm^2	-	f_y=350
Compressive strength N/mm^2	f_c=38	-
Tensile strength N/mm^2	f_{ct}=3.8	-

It is observed that up to a load of about 4kN, the response is found to be insensitive to the tension softening model. The analysis also indicated first cracking of the slab

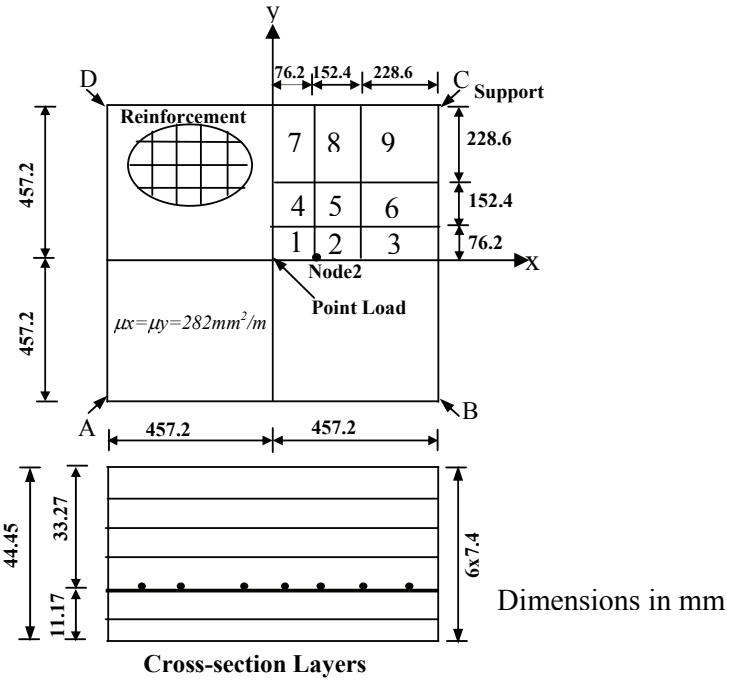

Figure 13: Plan and cross-section of McNeice slab

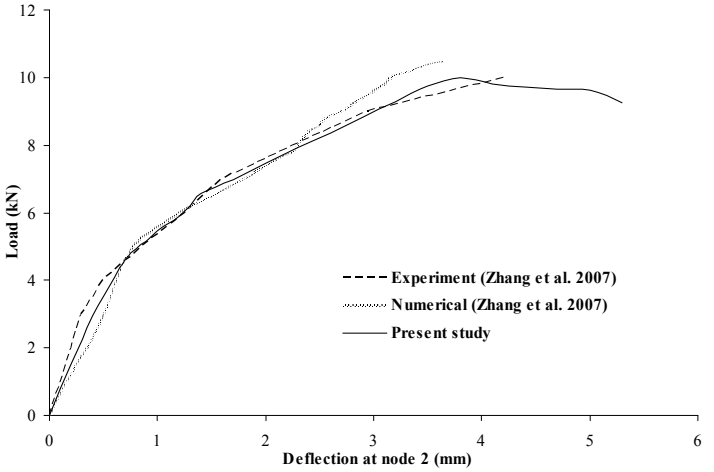

Figure 14: Load vs deflection for McNeice slab

around 4.8kN. However, no evidence is available to know about the appearance of first crack during the experiment. Extensive cracking was observed in the analysis at a load level starting from 45% of ultimate load. This is the stage where maximum crack propagation occurred. Fig. 15 shows the crack width in all the elements at 30%, 60% and 80% of ultimate load. At 30% of the ultimate load, only one element was found to have cracked while all elements showed cracks at 60% of ultimate load. At 80% of ultimate load, maximum crack width of about 0.16mm was observed in element 1, which is close to the load point.

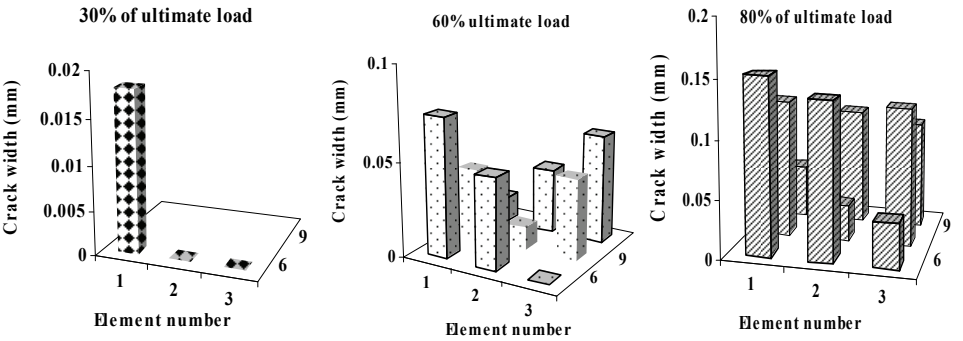

Figure 15: Crack width in McNeice slab at different load levels

Nonlinear relation between bond stress and slip of reinforcing bar in element 1 (highly cracked element) is shown in Fig. 16. A gradually increasing nonlinear behaviour can be observed from Fig. 16. Maximum bond stress is obtained as 3.39 MPa for a slip of 0.023 mm in the analysis.

6 Summary and Conclusions

The paper contributes a new constitutive model in stress-strain space to describe behaviour of concrete under tension. The model is proposed in a form applicable for nonlinear finite element analysis of RC structures. As per the model, concrete in uncracked state is described by linear relation while a bilinear relation is used to model the cracked concrete. An existing model of concrete for similar purpose but in stress-crack width space is used as basis to define the transition points of the proposed bilinear model. Delimiter for cracking response is prescribed by a strain-based criterion. By applying energy equivalence principle, a methodology is proposed to calculate crack width in service state of RC structures. Uniqueness of this methodology is in making use of strain to calculate the crack width instead of the usual average crack spacing which lacks clear physical meaning. The proposed

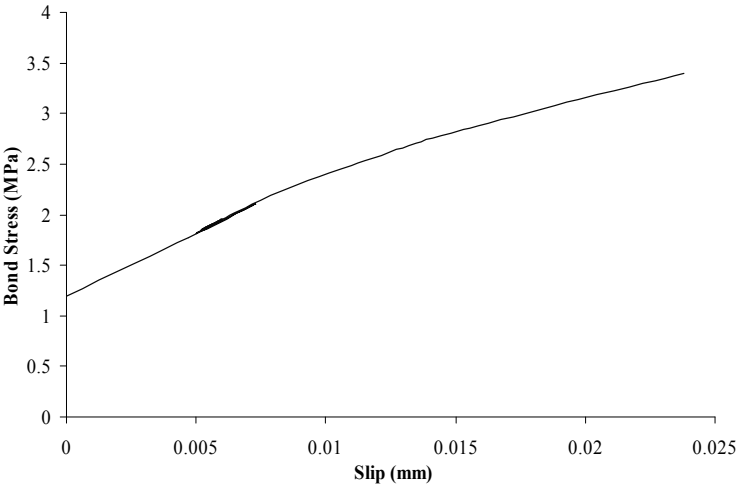

Figure 16: Slip vs bond stress for Mc Niece slab

crack width expression is well suited for application in a conventional nonlinear finite element analysis in which strains are commonly available as output. Constitutive model is integrated with a compatible crack representation theory which accounts for direction of the crack tip to evaluate the effective stiffness of a cracked member. As per this, crack tip is reoriented to remain always perpendicular to that of maximum principal stress. To enable this, thickness of the RC structure is modelled as layers with reinforcement smeared into some of them. Contribution of bond-slip to nonlinear behaviour of the RC structure is included by a simple relation available in literature.

Numerical application of the model and other associated features is demonstrated by analyzing a simply supported RC beam and McNiece slab over a large range of imposed load. In both the structures, experimentally measured responses are used to validate and bench mark the analysis output. Close match of the predicted load-deflection response of the beam with that of measured demonstrates the superior performance of the model even beyond the ultimate state. Simply supported beam is subjected to two point loading at $1/3^{rd}$ span length. Pure flexural behaviour of mid span of the beam is exploited to verify the predictability of the crack width model. Maximum crack width is found to differ by only about 10% with the corresponding measured value. Besides, the analysis is found to provide useful information about the nature of cracks in a RC structure. Predicted nonlinear response of McNiece slab for exactly the tested configuration again reiterates the superior performance of the model. For both the structures analysed, bond behaviour is

investigated by calculating the slip between concrete and reinforcing steel. This showed higher bond stress in near- and post-ultimate range for both the structures analysed and the same is also identified to be the one of the reasons behind the nonlinearity in load-deflection response.

Acknowledgement: The authors thank their colleagues Dr. G. S. Palani, Mr. A. Rama Chandra Murthy, and Dr. P. Kamatchi, Scientists, SERC for their valuable suggestions. This paper is being published with kind permission of the Director, CSIR-SERC.

References

ACI 318 (1984): *Building Code Requirements for Reinforced Concrete*, American Concrete Institute, Detroit.

ASCE (1982): State of the Art Report on Finite element analysis of Reinforced Concrete, Task Committee on Finite Element Analysis of Reinforced Concrete Structures, ASCE special publication, Washington, USA.

Assan, A. E. (2002): Nonlinear analysis of reinforced concrete cylindrical shells, *Computers and Structures*, 80(27-30), 2177-2184.

Au, F.T.K., Bai, Z.Z. (2007):, Two-dimensional nonlinear finite element analysis of monotonically and non-reversed cyclically loaded RC beams, *Engineering Structures*, 29(11), 2921-2934.

BS: 8110 British Standard, (1989):, *Structural Use of Concrete*- part 2, British Standards Institutions, London.

CEB-FIP (1990): *Model Code Design code lausanne committee*, Euro-International Du Beton, Bulletind, Information 195.

Cerioni, R., Iori, I., Michelini, E., Bernardi, P. (2008): Multi-directional modeling of crack pattern in 2D R/C members, *Engineering Fracture Mechanics*, 75(3-4), 615-628.

Cervera, M. (2008): An orthotropic mesh corrected crack model, *Computer Methods in Applied Mechanics and Engineering*, 197(17-18), 1603-1619.

Cho, J., Cho, N., Kim N., Choun, Y. (2003): Stress-strain relationship of reinforced concrete subjected to biaxial tension, Transactions of the 17^{th} International Conference on Structural Mechanics in Reactor Technology, Czech Republic, Prague, Aug 17-22, 1-9.

Chowdhury, S.H. (2001): Crack Width Predictions of Reinforced and Partially Prestressed Concrete Beams: A Unified Formula, *Structural Engineering, Mechanics and Computation*, 327-334.

Colotti, V., Spadea, G. (2005):, An analytical model for crack control in reinforced concrete elements under combined forces, *Cement and Concrete Composites*, 27(4), 503-514.

Eligehausen, R., Popov, E.P., Betrtero, V.V. (1983): Local bond stress-slip relationships of deformed bars under generalized excitations, Report No. UCB/EERC 83-23, Earthquake Engineering Research Center, University of California, Berkeley.

Frag, H.M., Leach, P. (1996): Material modelling for transient dynamic analysis of reinforced concrete structures, *Intl. J. Num. Meth. Eng.*, 39, 2111-2129.

Gomes, H.M., Awruch, A.M. (2001):, Some aspects on three-dimensional numerical modelling of reinforced concrete structures using the finite element method, *Advances in Engineering Software*, 32(4), 257-277.

Gupta, A.K., Akbar H. (1984): Cracking in RC analysis, *Jl. Struct. Eng., ASCE,* 110(8), 1735-1746.

Hayashi, S., Kokusho, S. (1985): Bond-behaviour in the neighborhood of crack, Proc. of the U.S-Japan Joint Seminar on Finite Element Analysis is of RC, Tokyo, Japan, 364-373.

Hillerborg, A., Modeer, M., Petersson, P.E. (1976): Analysis of crack formation and crack growth is concrete by means of fracture mechanics and finite elements, *Cement and Concrete Research*, 6, 773-782.

Hwang, S.K., Yun, H.D. (2004): Effects of transverse reinforcement on flexural behaviour of high-strength concrete columns, *Engineering Structures*, 26(1), 1-12.

IS-456 (2000): Plain and reinforced concrete- code of practice, Bureau of Indian Standards, New Delhi.

Kratzig, W.B., Petryna, Y.S., Noh, S.Y. (2004): Structural damage simulation and lifetime management for large natural draft cooling towers, Proc. of Intl. Conf. Natural Draught Cooling Towers, Istanbul, 371-379.

Lackner, R., Herber, A., Mang, H. (2003): Scale transition in steel-concrete interaction I: model, *J. Eng. Mech., ASCE*, 129(4), 393-402.

Marecki, T., Marzec, I., Bobiski, J., Tejchman, J. (2007): Effect of a characteristic length on crack spacing in a reinforced concrete bar under tension, *Mechanics Research Communications*, 34(5-6), 460-465.

Oliveira, R.S., Ramalho, M.A., Correa. M.R.S. (2008): A layered finite element for reinforced concrete beams with bond–slip effects, *Cement and Concrete Composites*, 30(3), 245-252.

Petersson, P.E. (1981): Crack growth and development of fracture zones in plain concrete and similar materials, Report TVBM-1006, Division of Building Materi-

als, Lund Institute of Technology, Lund, Sweden.

Ramtani, S., Berthaud, Y., Mazars, J. (1992):, Orthotropic behavior of concrete with directional aspects: modelling and experiments, *Nuclear Engineering and Design*, 133(1), 97-111.

Reinhardt, H.W., Cornelissen, H.A.W., Hordijk, D.A. (1986): Tensile tests and failure analysis of concrete, *J. Struct. Eng., ASCE*, 112(11), 2462-2477.

Roesler, J., Paulino, G.H., Park K., Dicke C. G. (2007): Concrete fracture prediction using bilinear softening, *Cement & Concrete Composites*, 29(4), 300-312.

Russo, G., Pauletta, M., Mitri, D. (2009): Solution of bond distribution in asymmetric RC structural members, *Engineering Structures*, 31(3), 633-641.

Theiner, Y., Hofstetter, Y.G. (2009): Numerical prediction of crack propagation and crack widths in concrete structures, *Engineering Structures*, 31(8), 1832-1840.

Vecchio, F.J., Collins, M. P. (1986): The modified compression field theory for RC elements subjected to shear, *J. ACI*, 83(6), 925-933.

Vidal, T., Castel, A., François, R. (2004): Analyzing crack width to predict corrosion in reinforced concrete, *Cement and Concrete Research,* 34(1), 165-174.

Xu, S. (2000): Determination of parameters in the bilinear, Reinhardt's nonlinear and exponentially nonlinear softening curves and their physical meaning, Institute of Construction Materials, University of Hamburg, Libri, Germany, 410-424.

Zienkiewicz, O.C., Taylor, R.L. (2000):, The Finite Element Method, Vol. I: The Basis, Vol. II: Solid Mechanics, Butterworth-Hieneman Ltd., Massachuchets.

Zhang, Y.X., Bradford, M.A., Gilbert, R.I. (2007): A layered cylindrical quadrilateral shell element for nonlinear analysis of RC plate structures, *Adv. Eng. Software*, 38, 488-500.